Monomer Dynamics in Double- and Single-Stranded DNA Polymers

Roman Shusterman, Sergey Alon, Tatyana Gavrinyov, and Oleg Krichevsky*

Physics Department, Ben-Gurion University, Beer-Sheva 84105, Israel

(Received 9 June 2003; published 29 January 2004)

We present the first measurements of the kinetics of random motion of individual monomers within large polymer coils. We use double- and single-stranded DNA (dsDNA and ssDNA) as models of semiflexible and flexible polymers, respectively. Fluorescence fluctuations of DNA fragments labeled specifically at a single position reveal the time dependence of the DNA monomer's mean-square displacement $\langle r^2(t)\rangle$. The monomer motions within dsDNA and ssDNA coils are characterized by two qualitatively different kinetic regimes: close to $\langle r^2(t)\rangle \propto t^{2/3}$ for ssDNA and $\langle r^2(t)\rangle \propto \sqrt{t}$ for dsDNA. While the kinetic behavior of ssDNA is consistent with the generally accepted Zimm theory of polymer dynamics, the kinetic behavior of dsDNA monomers is in good agreement with the Rouse model.

DOI: 10.1103/PhysRevLett.92.048303 PACS numbers: 82.35.Lr, 82.35.Pq, 82.37.–j, 87.15.He

The dynamical properties of polymers arise from the stochastic monomer motions which are subject to connectivity constraints within the polymer chain. The first theoretical description of random motions of monomers within an isolated polymer coil was presented by Rouse [1] as the classical beads-springs model. Rouse's model accounted for the entropic elasticity of polymer segments and the viscous friction of the solvent. Furthermore, it was recognized rather early that hydrodynamic interactions between the monomers play a major role in the polymer dynamics. These effects were incorporated by Zimm [2], whose theory is generally believed to hold for flexible polymers in the dilute regime [3].

Both Rouse and Zimm theories give a detailed description of the stochastic motion of monomers. However, classical dynamic light scattering experiments were able to resolve only the largest-scale dynamics, such as coil diffusion and the slowest modes of polymer shape fluctuations [4]. Indeed, since all of the monomers scatter light coherently, dynamic light scattering is mostly sensitive to the large collective motions of monomers. More detailed information on the kinetics of monomer motion in polymer melts has been revealed by neutron spin-echo spectroscopy [5]. New visualization and manipulation tools have allowed one to monitor large-scale shape relaxation of single DNA coils under different types of stresses [6,7].

Here, we present the first measurements of the stochastic motion of individual monomers within isolated polymer coils. We use single- and double-stranded DNA (ssDNA and dsDNA) as model polymers. While ssDNA is known to be a flexible polymer [8], dsDNA is a semiflexible polymer: the length characterizing its rigidity with respect to thermal fluctuations, or Kuhn length, $b \sim 100$ nm [$\sim$340 bp (base pairs)], is much larger than the dsDNA width $d \approx 2$ nm [9,10]. The statistics and dynamics of polymer fluctuations at the length scales below b are directly influenced by the polymer stiffness, and much of the interest in the dynamics of stiff polymers was focused on this regime, which is specific to semiflexible polymers [11–13]. For length scales larger than b, the statistical properties of semiflexible and flexible polymers are similar [14], and the dynamics of semiflexible polymers is predicted to be close to that of the flexible coils [15].

We attach a fluorescent label specifically to a single base on the long DNA molecules and monitor the motion of the labeled monomers with the fluorescence correlation spectroscopy (FCS) technique. We note that FCS has been used recently [16] to assess the general features of the internal dynamics of randomly labeled DNA coils. FCS [17,18] measures the diffusion kinetics of fluorescent species by monitoring the fluctuations $\delta I(t)$ in emission intensity $I(t)$ in a confocal illumination beam. As fluorescent molecules move in and out of the sampling volume, their fluorescence excitation and thus emission fluctuate: therefore the shape of the autocorrelation function of the fluorescence fluctuations $G(t) = \langle \delta I(0)\delta I(t)\rangle / \langle I(t)\rangle^2$ reflects the kinetics of diffusion. For independent point sources of fluorescence randomly moving in a Gaussian beam, $G(t)$ is directly related to the mean-square displacement (MSD) $\langle r^2(t)\rangle$ of the sources of fluorescence:

$$G(t) = \frac{1}{n}\left(1 + \frac{2}{3}\frac{\langle r^2(t)\rangle}{w_{xy}^2}\right)^{-1}\left(1 + \frac{2}{3}\frac{\langle r^2(t)\rangle}{w_z^2}\right)^{-1/2}, \qquad (1)$$

where w_{xy} and w_z define the dimensions of the sampling volume in lateral and transversal dimensions, respectively, and n is the average number of independently moving sources of fluorescence in the sampling volume.

We performed FCS measurements on freely diffusing ssDNA and dsDNA fragments of different lengths (from 2000 bp to 23 000 bp dsDNA, 2000 to 23 000 bases ssDNA) specifically labeled at their extremities by a single carboxyrhodamine 6G (Rh6G) fluorophore. In this case the fluctuations in fluorescence result from the motions of the DNA tagged end, and since the size of the DNA coils used in the experiment is comparable to

the dimensions of the sampling volume, $G(t)$ is sensitive to the monomer dynamics within a polymer.

Different dsDNA fragments (2400, 4400, 6700, 9400, and 23 100 bp) were obtained through digestion of Lambda DNA with HindIII endonuclease and then ligated to short synthetic oligonucleotides prelabeled with carboxyrhodamine 6G by reacting the succinimidyl ester of the dye onto the 3′-primary amino group of the oligonucleotide. The samples were repeatedly separated and purified with anion-exchange high-pressure liquid chromatography. The experiments on dsDNA were performed in 10 mM NaH_2PO_4, 1 mM EDTA (ethylenediaminetetraacetate), 0.1 M NaCl, pH 7.6 buffer at 20 °C. The measurements on ssDNA molecules were obtained by melting dsDNA samples in denaturing alkaline conditions. To ensure complete separation of the strands the measurements on ssDNA were performed in extreme alkaline buffer (50 mM Na_3PO_4, 1 mM EDTA, 0.3 M NaCl, pH 12.3) and at elevated temperature $T = 37$ °C [19]. The concentration of DNA was within the dilute regime and corresponded to 0.03 to 0.3 molecules in the confocal volume (0.5 fl) on average. The results were robust with respect to three- and tenfold dilutions as expected for the dilute regime.

Measurements were conducted in a homebuilt confocal FCS setup, similar to that described in [18]. Excitation was by 514 nm argon laser light at 10 μW focused by a Nikon 60× NA1.2W objective. For power of the excitation beam of up to 30 μW the results were not sensitive to the excitation intensity. The dimensions w_{xy} and w_z of the sampling volume were calibrated by measuring the diffusion of free Rh6G fluorophores [18].

We present two typical correlation functions measured for 6700 bp dsDNA and 6700 base ssDNA in Fig. 1. The main decay of the measured $G(t)$ in the millisecond scale characterizes the kinetics of monomer motion. At the shortest time scales (below 1 μs) there is an exponentially decaying process related to the internal dynamics of the fluorophore only: singlet-to-triplet state conversions [20]. These transitions are well separated in the time domain from the monomer motions, and we fit the triplet state dynamics below 1 μs with $Ae^{-Bt} + G(0)$ exponents in order to find the intercept $G(0) = 1/n$ in Eq. (1). Then, through Eq. (1), the MSD $\langle r^2(t)\rangle$ of a labeled monomer (i.e., end monomer) can be extracted from the measured $G(t)$.

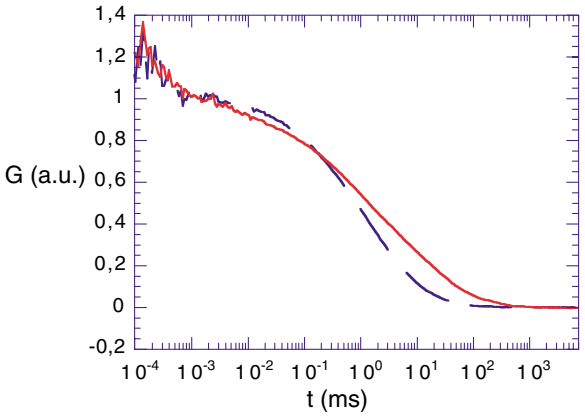

FIG. 1 (color online). FCS correlation functions for the end-labeled 6700 bp dsDNA fragment (red solid line) and 6700 base ssDNA (blue dashed line). To facilitate comparison, the correlation functions were normalized to have the same level ~1 at short time scales.

In Fig. 2 we present the monomer's MSD for 6700 bp dsDNA and 6700 base ssDNA fragments. The measurements span 5 decades in time, from ~3 μs to ~0.3 s. Two different regimes of motion can be clearly distinguished for each of the samples. At long time lags ($t > 5$ ms ssDNA; $t > 40$ ms dsDNA), $\langle r^2(t)\rangle$ is linear with time for both dsDNA and ssDNA: this regime corresponds to the monomer motions above the polymer coil size and reflects the trivial diffusion of the coil as a whole $\langle r^2(t)\rangle = 6D_G t$, where D_G is the diffusion coefficient of the polymer. The interesting regime occupies shorter time scales and corresponds to monomer motions within the polymer coil. In this regime, ssDNA and dsDNA exhibit profoundly different kinetic dependencies (Fig. 2): $\langle r^2\rangle \propto t^{0.50\pm0.01}$ for dsDNA, which is consistent with the prediction of the original Rouse model $\langle r^2\rangle \propto \sqrt{t}$, and $\langle r^2\rangle \propto t^{0.69\pm0.01}$ for ssDNA, which is close to the Zimm-model prediction $\langle r^2\rangle \propto t^{2/3}$.

The kinetics of internal motion for both dsDNA and ssDNA depends only weakly on the length of the polymer (Fig. 3), and thus the Rouse model and the Zimm-model behaviors appear to be generic to dsDNA and ssDNA internal dynamics, respectively. We note that for dsDNA

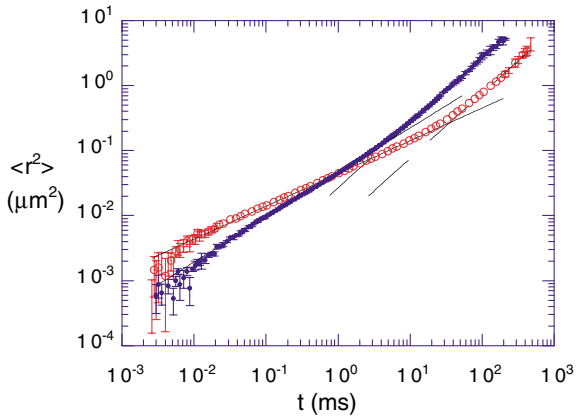

FIG. 2 (color online). The mean square displacement as a function of time for the end monomers of 6700 bp dsDNA fragment (red open circles) and 6700 base ssDNA (blue full circles) as extracted from measured FCS correlation functions. The long-time portion of the data corresponds to the diffusion of a polymer coil as a whole and $\langle r^2\rangle \propto t$ (dashed lines). The short-time data correspond to the monomer motion inside the coil. The best power fits $\langle r^2\rangle \propto t^{\alpha}$ to the low-time portion of the data give $\alpha = 0.50 \pm 0.01$ for dsDNA and $\alpha = 0.69 \pm 0.01$ for ssDNA (solid lines).

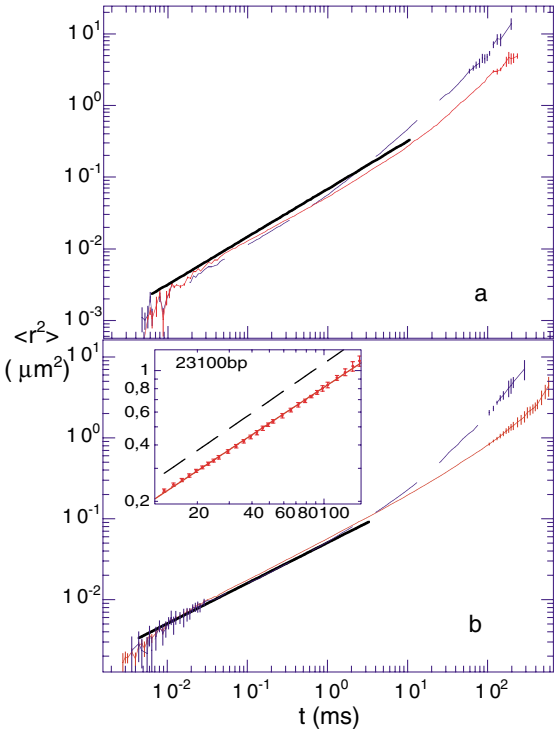

FIG. 3 (color online). The kinetics of random motion $\langle r^2(t)\rangle$ of the end monomer of ssDNA (a) and dsDNA (b) fragments of different lengths (in units of bases for ssDNA, base pairs for dsDNA): 2400 (blue dashed line) and 23 100 (red solid line). Thick solid lines are the theoretical predictions by (a) Zimm theory Eq. (4) and (b) Rouse model Eq. (3). Inset in (b): blowup of the data region for 23 100 bp dsDNA showing Zimm dynamics. Red solid line: the best power fit through these data ($\alpha = 0.64 \pm 0.01$); dashed line: Zimm dynamics given by Eq. (4) (with $\eta = 1$ mPa s at $T = 293$ K).

there are signs of an additional kinetic regime at the shortest time scales ($t < 20$ μs) corresponding to the motions below the Kuhn length ($\langle r^2\rangle < b^2 \approx 0.01$ μm^2). There the monomer dynamics should be directly influenced by the polymer stiffness [11,12,15]. However, in this range large experimental uncertainties prevent an accurate characterization of the kinetics.

Quantitatively, the predictions of the Rouse and Zimm models for MSD of the end monomer can be obtained by summation of the contributions of independent normal modes of polymer fluctuations [3]:

$$\langle r^2(t)\rangle = 6D_G t + \frac{4Nb^2}{\pi^2}\sum_{k=1}^{\infty}\frac{1-\exp(-t/\tau_k)}{k^2}, \qquad (2)$$

where the first term reflects the diffusion of the coil as a whole, the second term corresponds to the monomer motion within the coil, $N = L/b$ is the number of Kuhn segments b comprising the polymer length L, and τ_k is the relaxation time of the kth spatial mode. Substituting the relaxation times from [1,2] and evaluating the sum in Eq. (2), we have

$$\langle r^2(t)\rangle \approx \left(\frac{48b^2k_BT}{\pi\gamma}t\right)^{1/2} \qquad (3)$$

and

$$\langle r^2(t)\rangle \approx 2\left(\frac{k_BT}{\eta}t\right)^{2/3} \qquad (4)$$

for the end-monomer motion within the coil for the Rouse and Zimm models, respectively. Here η is the viscosity of the solvent and γ is the friction coefficient of the polymer segment of the Kuhn length b, which can be interpreted as that of a rod with length b and diameter d: $\gamma = 3\pi\eta b/\ln(b/d)$ [21]. We note that these formulas are just the equivalents of those obtained by Dubois-Violette and de Gennes [22,23] with a numerical factor difference stemming mainly from the difference in monomer position (end monomer as opposed to average monomer).

The agreement between the Rouse model prediction Eq. (3) (with known values of $b = 100$ nm, $d = 2$ nm for dsDNA, $\eta = 1$ mPa s at $T = 293$ K for aqueous solvent) and the experimental data on dsDNA is very good [Fig. 3(b)]. We find the agreement between the Zimm theory Eq. (4) and the results on ssDNA even more remarkable [Fig. 3(a)], since there are no polymer-dependent parameters entering the equation [$\eta = 0.69$ mPa s at $T = 310$ K were used in Eq. (4)], and thus the behavior in this regime should be universal for all polymers in similar solvent conditions.

While Zimm-type kinetics for ssDNA corresponds to the common view on polymer dynamics and, thus, could have been expected, the Rouse regime observed for dsDNA is puzzling. The fact that the hydrodynamic interactions are negligible over a wide range of monomer motion in dsDNA is apparently related to dsDNA semiflexibility. A large Kuhn length means that the distances between DNA segments are relatively large and, respectively, the hydrodynamic interactions between them are weak. The strength of the hydrodynamic interactions between the monomers is usually characterized by the "draining" parameter $h = N^{1/2}\gamma/(12\pi^3)^{1/2}b\eta$ [2]. For $h \ll 1$ the hydrodynamic interactions are weak and Rouse model behavior should be observed. For $h \geq 1$ hydrodynamic backflow effects dominate the polymer dynamics, which in this case should obey the predictions of the Zimm model. Since $h \propto \sqrt{N}$ one expects that with increasing polymer length the hydrodynamic interactions will become dominant. However, for monomer motion within dsDNA coils there are no signs of disappearance of Rouse regime kinetics with increasing polymer length. Quite the opposite, the range of the Rouse regime appears to grow as the coil size grows, and hence a larger range of motion within a coil is available [Fig. 3(b)].

However, a closer look [23] at hydrodynamic effects reveals that even for large draining parameters the dynamics of the high spatial frequency modes such that $k > h^2$ should agree with the Rouse model. These modes

can "deliver" the end monomer to the maximal displacement r_R, which can be found from Eq. (2):

$$r_R^2 = \frac{4Nb^2}{\pi^2} \sum_{k=h^2}^{\infty} \frac{1}{k^2} \approx \frac{16b^2}{3\pi h^2} \approx \frac{16b^2}{3\pi} \ln^2 \frac{b}{d}, \qquad (5)$$

where $\gamma = 3\pi\eta b/\ln(b/d)$ was substituted. Thus even if the large-scale dynamics of a long polymer is controlled by the hydrodynamic interactions, the motions at scales below r_R could be uninfluenced by those. The range of Rouse dynamics, from $\langle r^2(t)\rangle \sim b^2$ to $\sim r_R^2$, depends critically on the polymer flexibility, or b/d ratio. For a flexible polymer, such as ssDNA, $b \sim d$ and no appreciable Rouse regime exists. For dsDNA, $b/d \approx 50$ and the Rouse regime can occupy a rather wide range of MSDs: from $\sim b^2 \approx 0.01\ \mu\text{m}^2$ to $26b^2 \approx 0.26\ \mu\text{m}^2$ (but cannot of course exceed the polymer coil size $\sim Nb^2$), which is consistent with our observations [Fig. 3(b)].

For $\langle r^2(t)\rangle > r_R^2$ we expect to observe Zimm-type dynamics. For ssDNA it occupies all of the accessible range of motions. For dsDNA samples, apart from the longest ones, r_R is larger or close to the coil size, and thus for $\langle r^2(t)\rangle > r_R^2$ the regime of coil diffusion with $\langle r^2(t)\rangle = 6D_G t$ is expected. For the longest samples of 23 100 bp the coil size is $\sim Nb^2 \approx 68b^2 > r_R^2$, and Zimm-type dynamics can be observed, albeit in a limited range. Indeed, the best power fit [Fig. 3(b), inset] to the data in the 0.2 to 1.2 μm^2 range (10 to 200 ms time range) gives an exponent of 0.64 ± 0.01, close to Zimm's prediction of 2/3. Moreover, data in this range agree with Eq. (4) quantitatively. Thus despite the large differences in the internal structure and flexibility, both ssDNA and dsDNA obey a behavior close to the universal type predicted by Eq. (4).

Finally, we note that despite the relative success of the presented semiquantitative picture in explaining the data, our understanding of the experimental results is limited to the asymptotic behavior in the pure Rouse and Zimm regimes and to the crossover condition only. The detailed theories of semiflexible polymer dynamics [15] predict a crossover region so wide that no significant range of Rouse kinetics should be observed for reasonable values of parameters b and d. The reasons for this discrepancy between the theoretical predictions and the experimental results are not clear. Possibly, internal friction inside the DNA double helix (similar to Cerf friction [14]) has to be incorporated in the modeling.

To conclude, we have presented the first measurements of the kinetics of monomer random motion in isolated flexible (ssDNA) and semiflexible (dsDNA) coils. The internal motion in ssDNA is controlled by the hydrodynamic interactions between monomers and follows universal Zimm-model kinetics. In dsDNA, for a wide range of time scales (from 0.02 to 10 ms) the monomer motion appears to be uninfluenced by the hydrodynamic interactions and follows the Rouse-type dynamics. This regime does not disappear with increasing polymer length and thus is generic to dsDNA monomer motion. While the weakness of the hydrodynamic interactions can be attributed to dsDNA stiffness, the presence of the large range of Rouse-type kinetics appears to be in disagreement with current theories of polymer dynamics.

We are thankful to G. Altan-Bonnet, D. Chatenay, A. Meller, M. Elbaum, and R. Granek for illuminating discussions and critical comments to the manuscript. This work has been supported by Israel Science Foundation Grant No. 229/01-1.

*Electronic address: okrichev@bgumail.bgu.ac.il

[1] P. E. J. Rouse, J. Chem. Phys. **21**, 1272 (1953).
[2] B. H. Zimm, J. Chem. Phys. **24**, 269 (1956).
[3] M. Doi and S. F. Edwards, *The Theory of Polymer Dynamics* (Clarendon Press, Oxford, 1986).
[4] B. J. Bern and R. Pecora, *Dynamic Light Scattering* (Wiley, New York, 1976).
[5] A. Wischnewski, M. Monkenbusch, L. Willner, D. Richter, and G. Kali, Phys. Rev. Lett. **90**, 058302 (2003).
[6] T. T. Perkins, D. E. Smith, and S. Chu, Science **276**, 2016 (1997).
[7] P. S. Doyle, B. Ladoux, and J.-L. Viovy, Phys. Rev. Lett. **84**, 4769 (2000).
[8] S. B. Smith, Y. Cui, and C. Bustamante, Science **271**, 795 (1996).
[9] P. Cluzel, A. Lebrun, C. Heller, R. Lavery, J. L. Viovy, D. Chatenay, and F. Caron, Science **271**, 792 (1996).
[10] C. G. Baumann, S. B. Smith, V. A. Bloomfield, and C. Bustamante, Proc. Natl. Acad. Sci. U.S.A. **94**, 6185 (1997).
[11] L. LeGoff, O. Hallatschek, E. Frey, and F. Amblard, Phys. Rev. Lett. **89**, 258101 (2002).
[12] R. Everaers, F. Julicher, A. Ajdari, and A. C. Maggs, Phys. Rev. Lett. **82**, 3717 (1999).
[13] A. Caspi, M. Elbaum, R. Granek, A. Lachish, and D. Zbaida, Phys. Rev. Lett. **80**, 1106 (1998).
[14] P.-G. de Gennes, *Scaling Concepts in Polymer Physics* (Cornell University Press, Ithaca, London, 1993).
[15] L. Harnau, R. G. Winkler, and P. Reineker, J. Chem. Phys. **104**, 6355 (1996).
[16] D. Lumma, S. Keller, T. Vilgis, and J. O. Radler, Phys. Rev. Lett. **90**, 218301 (2003).
[17] D. Magde, E. Elson, and W. Webb, Phys. Rev. Lett. **29**, 705 (1972).
[18] R. Rigler, U. Mets, J. Widengren, and P. Kask, Eur. J. Biophys. **22**, 169 (1993).
[19] M. T. J. Record, Biopolymers **5**, 993 (1967).
[20] J. Widengren, U. Mets, and R. Rigler, J. Phys. Chem. **99**, 13 368 (1995).
[21] J. Riseman and J. G. Kirkwood, J. Chem. Phys. **18**, 512 (1950).
[22] P.-G. de Gennes, Physics (Long Island City, N.Y.) **3**, 37 (1967).
[23] E. Dubois-Violette and P.-G. de Gennes, Physics (Long Island City, N.Y.) **3**, 181 (1967).